JOURNAL OF CATALYSIS **168,** 143–153 (1997)
ARTICLE NO. CA971639

Hydrogenation Properties of Ruthenium Sulfide Clusters in Acidic Zeolites

Michèle Breysse,*[,1] Martine Cattenot,* Vassilios Kougionas,*[,2] Jean Claude Lavalley,† Françoise Mauge,† Jean Louis Portefaix,* and José Luiz Zotin*[,3]

*Institut de Recherches sur la Catalyse, 2 avenue Albert Einstein, 69626, Villeurbanne Cédex, France; and †Laboratoire Catalyse et Spectrochimie, URA 414-ISMRA, 6 boulevard Maréchal Juin, 14050, Caen Cédex, France

Received October 24, 1996; revised December 23, 1996; accepted December 23, 1996

Catalysts of ruthenium sulfide, dispersed in a series of Y zeolites with various acidic properties, were prepared by ion exchange and subsequent sulfidation. The activities for the reactions of hydrogenation of tetralin and toluene, carried out in the presence of H_2S (1.9%), vary widely according to the nature of the zeolites. Ruthenium sulfide catalysts are much more active when using acidic zeolite, HY and HYd (dealuminated), and a partially potassium-exchanged KHYd sample, than when using the KY support. The acidic properties of the sulfided RuY catalysts were determined *in situ* using infrared spectroscopy and the conversion of isooctane. Both methods gave similar rankings of catalyst acidity. The electronic properties of the ruthenium sulfide phase were examined by means of the infrared study of the adsorption of CO. A low-frequency shift of 15 cm^{-1} was observed for CO adsorbed on RuKY by reference to CO adsorbed on all other samples. The increase in activity for the hydrogenation of aromatics is related to the electron-deficient character of the sulfide particles in the acidic zeolites as has been proposed, in the literature, for metal catalysts. A superimposed influence of the acidic sites on the adsorption of the aromatic molecule may also occur which could explain the amplitude of the effect (difference of activity between the most and less active catalysts ~200 times) and the variations of activity observed within the series of the acidic catalysts.

INTRODUCTION

Zeolite-supported transition metal catalysts are widely applied in the petroleum and petrochemical industries. Several review articles dealing with these materials have been published. Among the most recent, Sachtler and Zhang have summarized the preparation of transition metal/zeolites and their properties in Ref. (1). A majority of these catalysts are bifunctional; i.e., besides the metal particles, the strong acid sites of the zeolite host are present. The traditional model for bifunctional catalysis assumes that metal sites provide the hydrogenation and dehydrogenation function, whereas the acid sites catalyze isomerization and cracking reactions. Besides this conventional role of both types of sites, it was observed experimentally, by several authors, that the hydrogenation properties of small Pt particles are anomalously high in acidic zeolite (2). In parallel, it was found that the activity of Pt in basic zeolites is reduced when the basicity of the support is increased (3, 4). Consequently, in these systems, the interaction of metal particles and protons has been studied for many years. The term "electron deficiency" was first introduced by Dalla Betta and Boudart (5) to account for these variations in properties of the Pt particles. The electron deficiency was ascribed to an electron transfer from small Pt particles to the zeolite and evidenced experimentally by X-ray absorption. Further evidence for a correlation between electron deficiency and proton concentration was found in FTIR studies of adsorbed CO (6).

By comparison to the numerous studies concerning metal particles in zeolites, only a few are related to the properties of sulfides. Nevertheless, NiMo sulfide is often associated with a HY zeolite in the composition of hydrocracking catalysts. Recently, the nature of NiMo phases encaged in HY zeolites was addressed by Leglise *et al.* (7, 8). Besides hydrocracking, the transition metal sulfides in zeolites could be utilized for hydrotreating reactions, i.e., hydrodesulfurization (9, 10), hydrodenitrogenation (11, 12) and the hydrogenation of aromatics (13). In several of these works the high activity of small clusters of transition metal sulfide in the pores of the zeolites was mentioned. The presence of acid sites seems to have a positive influence on the properties of these clusters at least for the hydrodesulfurization reaction (9, 14, 15). According to Welters (15), the reason for this synergetic effect between the metal sulfide and the acidic support may be an increased adsorption of thiophene

[1] Present address: Laboratoire de Réactivité de Surface, URA 1106, Université P. et M. Curie, 4 place Jussieu Casier 178, 75252, Paris Cédex, France. E-mail: breysse@ccr.jussieu.fr.

[2] Present address: National Technical University of Athens, Chemical Engineering Department, Section III, Materials Science and Technology, Zografou Campus, 9 Iroon Polytechniou street, 15780 Athens, Greece.

[3] Present address: Petrobras S.A., Cenpes/Dicat—Cidade. Universitaria—QD. 7, Ilha do Fundào, 21949-900 Rio de Janeiro, R.J. Brazil.

0021-9517/97 $25.00

in the pores of the zeolite, due to a strong adsorption on the acid sites. But Welters envisaged also other effects such as a change of the reaction pathway, or an alteration of the properties of the metal sulfide phase when dispersed in an acidic environment. In each case only the HDS activity of the metal sulfide particles located inside the zeolite pores will be increased by the presence of acid sites. Additionally, the acidic supports themselves also show a considerable initial activity, indicating that the acid sites are able to desulfurize thiophene (15).

Recently, we have shown that ruthenium sulfide can be dispersed as very small particles (~1 nm) located inside the zeolite framework (13, 16). Furthermore, we observed that these ruthenium sulfide clusters are highly active for the hydrogenation of aromatics even in the presence of a large amount of hydrogen sulfide. For these reasons, this system appears very well suited to study the properties of transition metal sulfide (TMS) clusters in zeolite and particularly the influence of acid sites. Other reasons for undertaking this study are related to the present environmental problems. Because the presence of aromatics in diesel fuels may contribute to air pollution, the reduction of their concentration is becoming ever more important and the design of new catalysts appears most desirable (17). It should be mentioned that the present hydrogenation catalysts proposed for this purpose by the catalyst manufacturers are often composed of group VIII metals in Y zeolites (18).

In the present study the question of whether or not the acid sites can improve the hydrogenating properties of ruthenium sulfide encaged in dealuminated and nondealuminated Y zeolites was investigated. The catalytic properties were determined in the hydrogenation of tetralin and toluene in the presence of about 1.9% of H_2S. The characteristics of the acid sites and of the hydrogenating sites were studied by IR spectroscopy. As a matter of fact, the hydroxyl groups of the zeolite are characterized by their OH vibrations. Moreover, the weak adsorption of CO on Brønsted acid sites can be used to determine the acidity of the protons. This probe molecule also provides information related to the electronic properties of the particles dispersed in the zeolites. CO adsorption experiments were performed at 100 K on sulfided samples activated *in situ*. This low temperature was chosen to avoid any modification of the active phase by the probe molecule adsorption. Nevertheless, these experimental conditions are far away from those utilized during the catalytic hydrogenating tests which are carried out under hydrogen pressure and in the presence of H_2S which may modify the concentration and strength of the acid sites. It is the reason why a model reaction, the hydrocracking of isooctane, was used to characterize the acid properties under conditions close to those of the aromatic hydrogenation (presence of hydrogen sulfide and similar temperature range). In a comprehensive study of the model reactions which can be employed for the characterization of acid sites, Bourdillon *et al.* (19) showed that the conversion of 2,2,4-trimethylpentane required acid sites of moderate strength which could be present on all the catalysts studied.

EXPERIMENTAL

Catalysts

The various zeolites utilized for this study are listed in Table 1, which also gives their main characteristics determined by chemical analyses, ^{29}Si solid-state NMR, and X-ray diffraction. KY and HY zeolites were prepared from NaY, supplied by Union Carbide (Type LZ-Y52), by two successive ion exchanges in an aqueous solution of KNO_3 (1 *M*) and NH_4Cl (1 *M*) at 333 and 293 K, respectively, for 24 h. A commercial dealuminated HYd zeolite supplied by Conteka (overall Si/Al = 6) was also utilized. Dealuminated zeolite KYd was prepared from this last support by two successive exchanges, in an aqueous solution of KNO_3 (1 *M*) at 333 K. As it was mentioned in our previous study related to ruthenium sulfide dispersed in KYd zeolite (13) the percentage of K obtained (~3%) is lower than that expected from the framework Si/Al ratio. This is related to the high proportion of extra framework aluminum species present in the starting HYd zeolite, as indicated by the chemical and NMR Si/Al ratios given in Table 1.

TABLE 1

Chemical Composition and Lattice Parameter of the Supports Used

Support	Chemical analysis (wt%)				Si/Al		a_0[c] (nm)	Unit cell
	Si	Al	Na	K	Chem[a]	Network[b]		
HY	36.1	12.8	0.9	—	2.7	2.4	2.475	$Na_4H_{52}(AlO_2)_{56}(SiO_2)_{136} \cdot xH_2O$
KY	27.4	10.4	0.2	14.7	2.6	2.4	2.473	$NaK_{55}(AlO_2)_{56}(SiO_2)_{136} \cdot xH_2O$
HYd	39.1	6.5	0.1	—	5.8	12.0	2.435	$H_{15}(AlO_2)_{15}(SiO_2)_{177} \cdot xH_2O$
KHYd	40.5	6.3	0.1	3.0	6.2	12.0	2.437	$K_9H_6(AlO_2)_{15}(SiO_2)_{177} \cdot xH_2O$

[a] The Si/Al atomic ratio was determined by chemical analysis.
[b] The Si/Al atomic ratio was determined by solid-state NMR of ^{29}Si.
[c] The lattice parameter was determined by X-ray diffraction.

TABLE 2

Chemical Composition of the Catalysts

Catalyst	K[a]	Ru[a]	Si/Al[b]
RuHY	—	3.2	—
RuKY	10.0	3.3	2.6
RuHYd	—	1.9	5.7
RuKHYd	0.8	1.8	5.8
Ru/Al_2O_3	—	6.8	—

[a] Chemical composition in wt%.
[b] Overall Si/Al atomic ratio.

Consequently, this support is more properly referred to as KHYd.

Supported ruthenium catalysts were prepared by means of ion exchange by stirring zeolite KY, HY, HYd, or KHYd in an aqueous solution of $[Ru(NH_3)_6]Cl_3$ (supplied from Johnson–Matthey), at room temperature for 48 h. The catalysts were washed with water three times and then air-dried overnight at 393 K. These samples are referred to, in the following, as RuKY, RuHY, RuKHYd, and RuHYd. The same amount of Ru was introduced in the exchange solution but the concentration of Ru (Table 2) is much lower for dealuminated zeolites (about 1.8 wt%) than for nondealuminated ones (about 3.3%). This may be ascribed to the restricted accessibility of some protons and potassium cations for ruthenium exchange due to the presence of extra-framework aluminum species or to the lower concentration of exchange sites in the dealuminated samples and presumably to the larger distance between neighbor exchange sites (at framework centered tetrahedra). The various samples were sulfided using gas flows of 15% of H_2S in H_2 at atmospheric pressure. The temperature of the reactor was gradually increased at a rate of 10 K min^{-1} up to 673 K at which temperature it remained for 4 h. The catalyst was cooled down to room temperature under the same sulfiding atmosphere and flushed with N_2 for 30 min. The Si/Al ratios determined by chemical analysis for the zeolites exchanged with ruthenium are very close to the values obtained for the starting zeolites which indicates that there is no change in the overall composition of the zeolites. For the sulfided samples the ^{29}Si NMR gave results comparable to those of Table 1 for RuKY, RuKHYd, and RuHYd but for RuHY the Si/Al ratio was modified. It increased from 2.4 for the initial HY support to 3.1 for nonsulfided RuHY and 4.1 after sulfidation. This dealumination process which appeared mainly after H_2S treatment may be compared to the dealumination process of zeolite by treatment with water vapor. Simultaneously for this last sample the crystalline fraction decreased from 98 to 30% whereas it remained high for the other catalysts. As expected the dealuminated samples appeared very stable during all the treatments. Exchange by K^+ enhanced also the stability to the H_2S treatment.

For purposes of comparison, a ruthenium on alumina catalyst containing 6.8% of Ru was also prepared using a preparation procedure described in Ref. (20). A γ alumina sample (BET surface area 236 $m^2\ g^{-1}$) in the form of extrudates was crushed and sieved to obtain a grain diameter range of 0.08–0.125 mm. The outgassed carrier was contacted with a solution of $RuCl_3$, $3H_2O$ (Aldrich Chemie) and sulfided using a gas flow of 15% of H_2S in N_2 because it was shown that this sulfiding procedure gives better results than the sulfidation under a H_2S–H_2 mixture (20). A commercial $NiMo/Al_2O_3$ hydrotreating catalyst containing 9% of Mo and 2.4% of Ni on γ-Al_2O_3 was utilized as reference. This catalyst was sulfided similarly as the RuY samples. An unsupported RuS_2 catalyst (21) was utilized in mechanical mixture with the RuY catalysts for the isooctane conversion.

Characterization

High-resolution electron microscopy (HREM) was used to determine the particle sizes and the location of ruthenium sulfide. Ultrathin slices (~20 nm) cut by ultramicrotomy of sample grains were examined in a JEOL 100 CX instrument.

EXAFS measurements were carried out for some of the samples as described in Ref. (13).

For infrared spectroscopy characterization, the samples were pressed into self-supporting discs (5 $mg \cdot cm^{-2}$). The catalysts were presulfided under gas flow *ex situ* as described above and further resulfided *in situ* in a low-temperature infrared transmission cell equipped with double walls with a space for coolling agent. For the *in situ* activation, the sample was first treated under vacuum and its temperature increased at a rate of 0.15 $K \cdot s^{-1}$ from room temperature to 523 K, at which temperature it was maintained for 30 min. Then, 80 Torr of a mixture of H_2S (15% vol.) and H_2 was introduced and the temperature was increased at a rate of 0.17 $K \cdot s^{-1}$ up to 673 K and maintained for 1 h. The sulfidation was repeated three times, each sulfidation step being followed by an evacuation at 523 K. For comparison, some samples were not sulfided and only treated by H_2.

Before infrared spectra were recorded, the cell was cooled at a temperature of about 100 K by using liquid nitrogen as coolant. The introduction of 0.5 Torr of helium in the cell allowed a better thermal contact between the sample and the cooled walls to be achieved. CO was purified by trapping at liquid nitrogen temperature before admission. Successive small doses of CO were introduced in the cell until a maximal pressure of 5 Torr.

Catalytic Activity Measurements

Experiments were carried out in high pressure and atmospheric pressure microreactor systems and operated in the dynamic mode in the gas phase. All the compounds were used nondiluted by a solvent and were introduced to

TABLE 3

Experimental Conditions Utilized for Catalyst Testing

Reaction	Experimental conditions				
	P_{H_2} (MPa)	Temperature (K)	P_{H_2S} (kPa)	$P_{reactant}$ (kPa)	Total flow rate (ml/min)
HC isooctane	0.1	573	2.5	2.3	40
HYD toluene	4.5	553–663	84.4	5.0	320
HYD tetralin	4.5	523–573	84.4	2.7	320

the reactor by means of a gas phase saturator. The experimental conditions, depending on the nature of the reacting molecule, are described in Table 3. For the above reactions the low conversions ($\leq$15%) used in the catalytic tests permit the application of a differential model for the determination of the rates of the reaction.

RESULTS

Nature of the Active Phase and Its Dispersion Determined by HREM and EXAFS

In a recent paper the nature of ruthenium sulfide clusters encaged in one of the supports of the present series, i.e., KHYd zeolite, was determined by electron microscopy (STEM-EDX and TEM) and EXAFS (13). Using a H_2S/H_2 mixture as sulfiding agent, it was shown by electron microscopy that the active phase consisted of small spherical particles ($\sim$1 nm) of a ruthenium sulfide-like phase homogeneously dispersed within the grains of the zeolite. The sulfur to ruthenium ratio of the ruthenium sulfide aggregates, evaluated by several techniques, chemical analyses, TPR, and EDX, was about 1.7, lower than the S/Ru ratio corresponding to RuS_2. EXAFS data of this sample were compared to those obtained with reference solids, i.e., unsupported RuS_2 and a Ru foil. Ru–S bonds, at a distance slightly lower than in the unsupported RuS_2 reference catalysts, were observed but also some Ru–Ru bonds corresponding to ruthenium metal. Taking into account the mean coordination number of the ruthenium atoms by sulfur, i.e., 5.1 for RuKHYd and 6 for RuS_2, and the mean coordination number of the ruthenium atoms by ruthenium in the metal-like phase, i.e., 3.5 for RuKHYd instead of 12 for Ru metal, a modeling of the EXAFS and HREM results was proposed.

The representation which emerges from these various studies is a cluster of a ruthenium sulfide-like phase (truncated octahedron structure) with very small domains of ruthenium metal located on a face of the octahedron. The model which fits the best with the experimental result corresponds to an overall amount of 38 atoms of Ru involved in the ruthenium sulfide-like phase with less than 10 Ru atoms in the bidimensional metal domain.

Similar experiments were carried out with all the ruthenium sulfide samples dispersed in the zeolites of the present study. Whatever the support, no noticeable differences were observed and the above results can be extended to all the catalysts.

The size of the metal domains is related to the H_2S partial pressure present in the atmosphere surrounding the catalysts. The above results were obtained after the sulfiding step carried out in the presence of 15% of H_2S in H_2. After catalytic tests, in experimental conditions similar to those utilized for the tetralin hydrogenation of the present study (1.85% of H_2S), the size of the metal domain slightly increased (the Ru–S coordination number decreased from 5.1 to 4.7 and the Ru–Ru coordination number increased from 3.5 to 5.1) and the crystallographic model suggested that about 13 Ru atoms are involved in a metal phase in close interaction with the ruthenium sulfide particle.

Infrared Spectroscopy

1. RuKY. Figure 1 shows the IR spectra in the OH stretching range of the series of RuY zeolites. The RuKY zeolite essentially presents two bands at 3654 and 3557 cm^{-1}. The high-frequency band (HF) characterizes hydroxyl groups situated in the supercages while the low-frequency band (LF) is specific to OH groups situated in sodalite cages or hexagonal prisms. The weak band at 3746 cm^{-1} is related to the presence of a small amount of Si–OH groups.

When small doses of CO are introduced at 100 K on the activated zeolite, only a few of the HF hydroxyl groups are

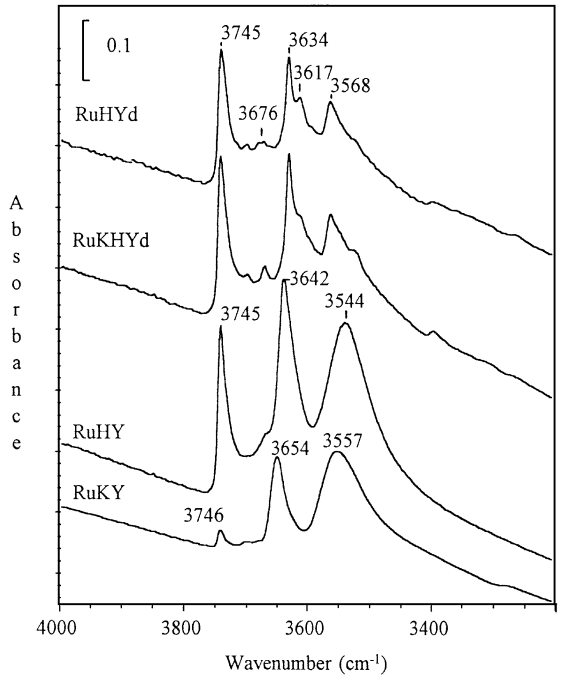

FIG. 1. IR spectra of the hydroxyl group vibration zone of the various Ru zeolites.

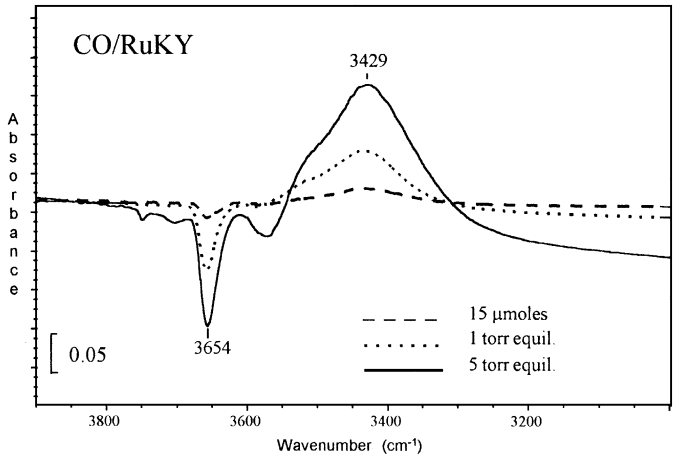

FIG. 2. Effect of CO adsorption on hydroxyl bands of RuKY. Difference spectra, after CO adsoption minus before.

affected (Fig. 2). Their frequencies are shifted toward lower wavenumbers, indicating an interaction with CO by hydrogen bond. The larger the wavenumber shift, the more acidic the hydroxyl groups. In the case of the RuKY, the $\Delta\nu$(OH) frequency shift is low (225 cm^{-1}), suggesting that the acidic strength of the HF hydroxyl groups is weak. This explains the small amount of HF hydroxyl groups perturbed by introducing small doses of CO. The introduction of a larger amount of CO affects a greater number of HF hydroxyl groups showing that they are accessible to CO but only weakly acidic.

In the ν(CO) stretching zone, the introduction of small doses of CO gives rise to a strong band at 2159 cm^{-1} (Fig. 3). Its intensity is not related to the decrease of the OH band at 3654 cm^{-1}. This suggests that the 2159 cm^{-1} band is essentially due to CO adsorption on K^+. Moreover, Maache (22) provided evidence for a relation between the $\Delta\nu$(OH) frequency shift when adsorbing CO and the ν(CO) frequency resulting from the hydrogen bond interaction. To a 225 cm^{-1} $\Delta\nu$(OH) shift must correspond a ν(CO) band near 2165 cm^{-1}. The detection of this band is probably prevented by the presence of the intense band at 2159 cm^{-1}; this confirms that the intensity of the ν(CO) band characterizing the hydrogen-bonded species is very weak.

When larger amounts of CO are introduced ($P = 5$ Torr) additional bands are observed at 2140 cm^{-1} (shoulder) and 2123, 2109, and 2051 cm^{-1} (broad) with a shoulder near 2005 cm^{-1} (Fig. 3). That at 2140 cm^{-1} is characteristic of physisorbed CO. The two bands at 2123 and 2109 cm^{-1} are also observed on KY zeolite without ruthenium. They could be assigned to CO adsorption on zeolite basic sites as already reported by Gruver and Fripiat (23). After evacuation ($P = 4 \times 10^{-5}$ Torr) at low temperature, the band at 2056 cm^{-1} with the weak shoulder near 2005 cm^{-1} mainly remains; it characterizes CO adsorption on ruthenium sites.

CO adsorption at room temperature detects only ruthenium adsorption sites since the only band observed is situated at 2048 cm^{-1} with a shoulder near 1986 cm^{-1} (Fig. 3). Its intensity is higher than that observed at low temperature in the same frequency range. In order to prevent any redispersion effect, as was suggested by Hadjiivanov *et al.* (24) for metallic Ru particles supported on titania, CO adsorption was performed at low temperature for the other catalysts of the series.

2. RuHY. The spectrum in the hydroxyl range is similar to that observed in the case of RuKY (Fig. 1). However, (i) the silanol band is much more intense, (ii) the wavenumbers of the HF and LF bands are lower (3642 and 3544 cm^{-1}, respectively) which may be attributed to an increase of strength of the Brønsted acidity in RuHY, and (iii) the intensities of HF and LF bands are stronger.

The acidity increase is confirmed by the ν(OH) shift of HF hydroxyls caused by CO adsorption: $\Delta\nu(OH) = 302$ cm^{-1} (Fig. 4). The corresponding ν(CO) frequency is

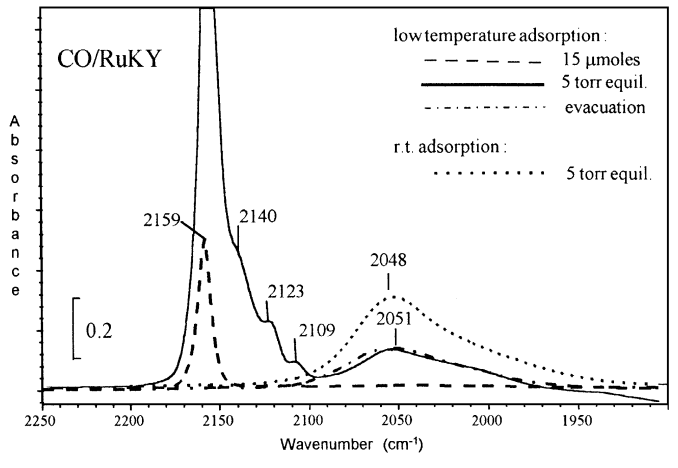

FIG. 3. IR spectra of CO adsorbed on RuKY.

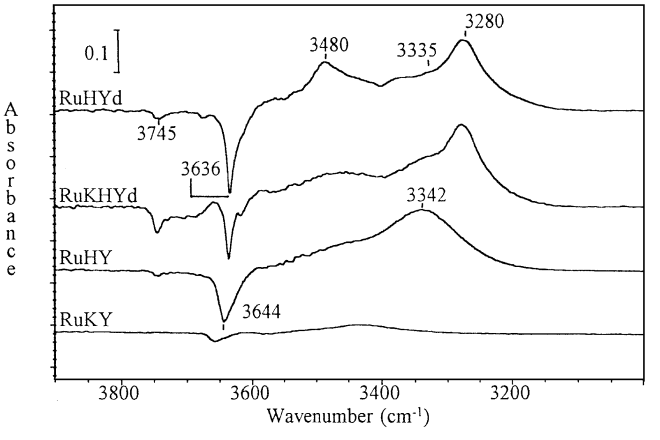

FIG. 4. Comparison of the effect of CO adsorption (15 μmoles) on the ν(OH) vibrations for the various Ru zeolites.

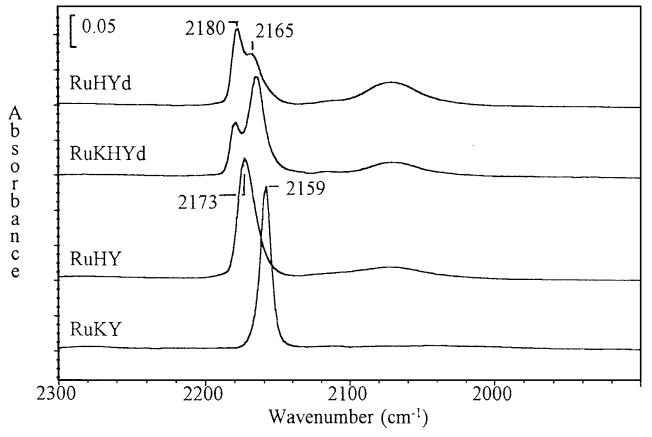

FIG. 5. Comparison of the IR spectra (15 μmoles) on the various Ru zeolites.

situated at 2173 cm^{-1} (Fig. 5), in nice agreement with that expected from the $\Delta\nu$(OH) shift (25).

The introduction of a higher amount of CO at 100 K ($P = 5$ Torr) leads, for $\nu < 2150$ cm^{-1}, to the appearance of numerous physisorbed species (band at 2140 cm^{-1}) and of a broad band at 2077 cm^{-1}, assignable to CO adsorption on Ru sites. Only this last band remains after evacuation at low temperature and is then observed at 2071 cm^{-1} (Fig. 6).

3. RuKHYd and RuHYd. Close results are observed on both samples. The range 3800–3500 cm^{-1} is complex and presents at least five bands: 3745ν(SiOH), 3676 (weak), 3634 (HF), 3617, and 3568 cm^{-1} (LF) (Fig. 1). CO adsorption at low temperature affects part or some of them and ν(OH)-perturbed bands are observed at 3280, 3335, and 3480 cm^{-1} (Fig. 4). The first band corresponds to the perturbation of HF hydroxyl groups ($\Delta\nu$(OH) = 356 cm^{-1}).

In the ν(CO) range, two bands mainly appear at 2180 and 2165 cm^{-1} (Fig. 5). That at 2180 cm^{-1} obviously characterizes CO adsorption on the most acidic HF hydroxyls. Its wavenumber is in good agreement with the perturbation in the ν(OH) zone and corresponds to a band at 3280 cm^{-1}. The ν(CO) band at 2165 cm^{-1} would correspond, in the case of RuHYd to OH groups giving rise to a $\Delta\nu$(OH) shift of about 200 cm^{-1}. This suggests that the ν(OH) band near 3335 cm^{-1} may be related to the perturbation of LF OH groups at 3568 cm^{-1}. However, this band at 3335 cm^{-1} and the band at 3480 cm^{-1} may also correspond to the perturbation of hydroxyl groups of amorphous silico-aluminate phases (24). In the case of RuKHYd, the intensity of the 2165 cm^{-1} band is stronger which shows that it is also due to CO adsorption on K^+ ions.

In the range below 2150 cm^{-1}, in addition to the band characterizing physisorbed CO species, a broad absorption band is noted near 2071 cm^{-1}. It persists after evacuation at low temperature and presents, in such conditions, a weak shoulder near 2110 cm^{-1} (Fig. 6).

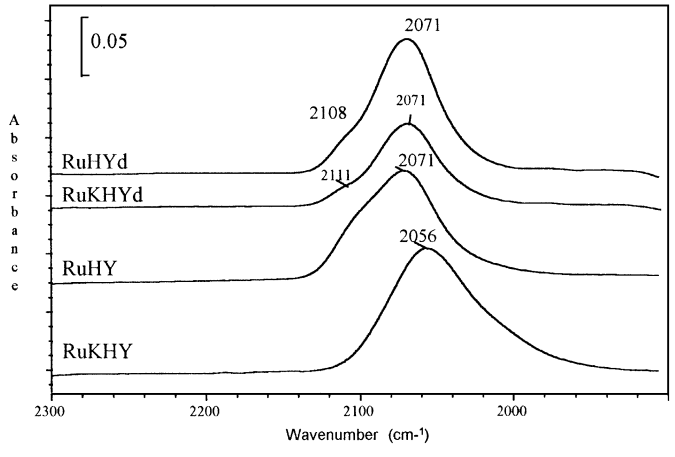

FIG. 6. Comparison of the IR spectra of CO adsorbed and evacuated at low temperature on the various Ru zeolites.

4. Reduced catalyst. Treated only by H_2, all the catalyst spectra present bands due to the perturbation of the ν(OH) zone by CO adsorption and bands of CO adsorbed on H^+ or K^+ sites similar to those obtained after sulfidation. Nevertheless on Ru sites, ν(CO) bands are shifted toward lower wavenumbers by comparison to the above results. The frequency values are compiled in Table 4.

5. Interpretation. Low-temperature CO adsorption followed by FTIR spectroscopy provides information on both the Brønsted acidity and the ruthenium state. Concerning the Brønsted acidity, the ν(OH) bands shift and ν(CO) wavenumbers, reported in Table 4, are consistent and show that the strength of Brønsted acidity decreases in the following order:

$$\text{RuHYd} = \text{RuKHYd} > \text{RuHY} \gg \text{RuKY}.$$

RuHYd presents a larger amount of strong Brønsted acid sites than RuKHYd, determined from the intensity of the 2180 cm^{-1} band (Fig. 5), which confirms that some K^+ ions in this latter sample are situated in cationic positions. These results are in agreement with literature data: the strength of Brønsted acid sites increases by dealumination (26). However, no very strong acid site is observed in $RuHY_d$ or $RuKHY_d$, despite that they are both dealuminated since no perturbed OH band is clearly evidenced below 3250 cm^{-1} (27). As for K^+ cations, it appears that the Lewis acidity they induce is stronger when the zeolite is dealuminated (ν(CO) = 2165 cm^{-1} in RuKHYd instead of 2159 cm^{-1} in RuKY).

Considering CO adsorption on Ru sites, the ν(CO) frequency gives information on the oxidation state of Ru sites: the higher the ν(CO) frequency, the lower the back-donation of the d electrons, and the most oxidized the ruthenium sites are. In order to keep constant the density of CO adsorbed and consequently the static and dynamic

TABLE 4

Wavenumbers and Wavenumber Shifts Resulting from CO Adsorption on the Different Sites

Samples	ν(OH) band shift (cm^{-1}) due to CO adsorption	ν(CO) wavenumber (cm^{-1}) resulting from adsorption on			
		H^+	K^+	Sulfided Ru	Reduced Ru
RuKY	225	2165 (weak)	2159	2056	2051
RuHY	302	2173		2071	—
RuKHYd	356 + 200	2180 + 2165	2165	2071	2063
RuHYd	356 + 200	2180 + 2165		2071	2063
Ru/Al_2O_3	—	—	—	2052	2026

interactions which modify the ν(CO) wavenumber, the results are compared after the following process: introduction of a large excess of CO at low temperature, and then evacuation at the same temperature (Fig. 6). The wavenumbers of ν(CO) bands characterizing the ruthenium sites of sulfided catalysts, measured under such conditions, are summarized in Table 4, and compared to those observed after H_2 reduction. It clearly appears that the ν(CO) wavenumber is always higher after treatment by $H_2S + H_2$ than by H_2 alone, indicating that the ruthenium sites on sulfided catalysts are not present as Ru^o. However, it is difficult to specify their oxidation state. It is worthwhile noticing that for a same treatment the results obtained on RuHYd and RuKHYd are similar (sulfided $\nu(CO) = 2071\ cm^{-1}$, reduced $\nu(CO) = 2063\ cm^{-1}$) whereas the ν(CO) band observed on RuKY is definitively lower (sulfided $\nu(CO) = 2056\ cm^{-1}$; reduced $\nu(CO) = 2051\ cm^{-1}$). This does not mean that ruthenium present in RuKY is easier to reduce since the same shift ($6\ cm^{-1}$) is observed when the catalysts are treated by $H_2 + H_2S$ compared to treatment by H_2 alone, whatever the sample. It is why we prefer to interpret the modifications of the ν(CO) wavenumber by electronic transfers between the zeolite and the Ru particles. Such effects have already been considered on metal in zeolites, for instance, by de Mallmann and Barthomeuf (28). In agreement with the literature, we observed that the stronger the acidity of the zeolite, the higher the ν(CO) frequency characterizing the Ru sites.

These results are compared to previous results obtained on sulfided or reduced Ru/Al_2O_3 (Table 4) where the interaction between the particles and the support is weak (29). For a same treatment, ν(CO) wavenumbers are definitively lower on Ru/Al_2O_3 ($2052\ cm^{-1}$) than on RuY samples, whatever the zeolite.

Hydrocracking of Isooctane

The hydrocracking of 2,2,4-trimethylpentane (isooctane) was used as a measure of the catalyst acidity by Bourdillon *et al.* (19). The conversion of this molecule in which tertiary carbocations intervene gives mainly isobutane and isobutene according to

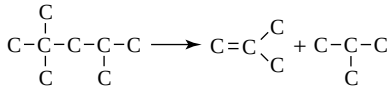

The cracking of secondary carbocations resulting from the isooctane isomerization is less observed:

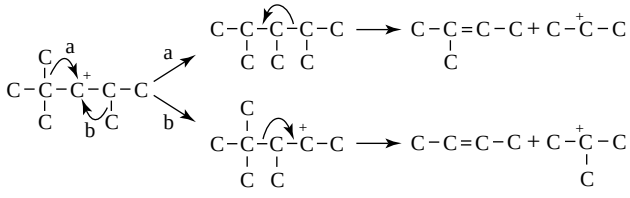

This reaction is less demanding than the conversion of other alkanes such as 2,4-dimethylpentane, 2-methylpentane, or *n*-hexane and requires Brønsted acid sites of medium strength. The authors observed also a very fast deactivation due to coke formation by dehydrogenation, cyclization, and further alkylation processes.

Under the experimental conditions used in the present work, 573 K, atmospheric pressure, and partial pressures of isooctane and H_2S of 2.3 and 2.5 kPa, respectively, the majority of the products observed were isobutane, some isobutene, and small quantities of propane and C_5 hydrocarbons. These products correspond well to those supposed to be formed by the reaction mechanisms proposed above.

Because of the rapid deactivation of all catalysts (Fig. 7) it is difficult to measure the true initial rate of isooctane disappearance which is the only representative of the catalyst acidity. On the other hand the correct characterization of the acidity of bifunctional catalyst implies that the hydrogenation–dehydrogenation capacity of the catalyst should be sufficient compared to its acidity so that the cracking reaction steps proceeding via carbonium ions are the rate limiting ones. As was observed by Leglise *et al.* (7), the hydrogenation function of a NiMo sulfide dispersed in HY zeolites is insufficient to allow ideal hydrocracking of heptane, the dehydrogenation step staying far under equilibrium; it was suspected that this could be also observed

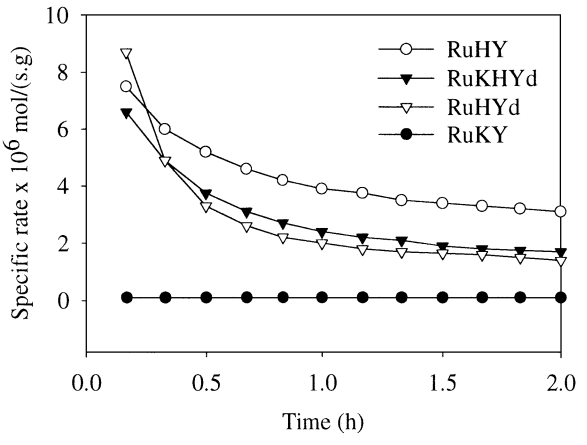

FIG. 7. Isooctane conversion rates for the sulfided RuY samples.

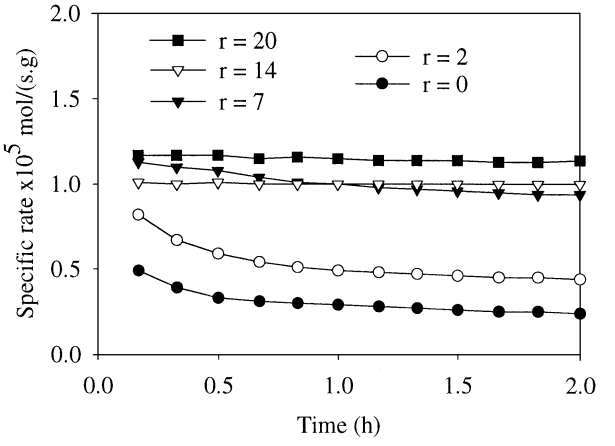

FIG. 8. Isooctane conversion rates for mixtures of RuKHYd and RuS_2 as a function of the weight ratio RuS_2/RuKHYd.

with the present catalyst. If this is the case, the addition of a hydrogenating–dehydrogenating catalyst would increase the overall rate until a value for which the rate of the cracking reaction would be the limiting one. For this purpose, unsupported RuS_2 was chosen since this catalyst is one of the most active transition metal sulfides for hydrogenation reactions (21). As a matter of fact, the utilization of metal catalysts cannot be envisaged due to their poor properties in the presence of the high partial pressure of H_2S present in the reacting mixture. On the other hand, it was shown that RuS_2 presents no acidic properties which can alter the results (Table 5).

Experiments were performed by mixing RuY catalysts with unsupported RuS_2, at different weight fractions. These results are shown in Fig. 8. It can be seen from this figure that the rate of isooctane disappearance increases with increasing the weight ratio of RuS_2/RuY from 0 to 14, indicating that the hydrogenation–dehydrogenation step is the rate limiting one when no RuS_2 was added. Weight ratios higher than 14 do not affect the value of the rate, indicating that the reaction steps involving carbonium ions become the rate limiting ones. A weight ratio of RuS_2/RuY = 20 was used for all the following tests in order to provide a sufficient hydrogenation function to the catalysts. The addition of a hydrogenation function also has the advantage of practically eliminating the deactivation of the catalysts due to coke poisoning (Fig. 9). The amount of RuS_2 which is required to balance the acidic function is very high. However, in such mechanical mixtures the hydrogenation sites of the unsupported catalyst are not utilized efficiently, being too far away from the acid sites of the zeolites. Although ruthenium sulfide is the most active among the transition metal sulfides for the hydrogenation of aromatics, its activity is much lower than that of a noble metal catalysts. This explains why notwithstanding the very good hydrogenating properties of ruthenium sulfide catalysts dispersed in Y zeolites, by comparison to other sulfides catalysts, the amount of active phase is probably too low to balance the acidic properties. A higher amount of ruthenium sulfide dispersed

TABLE 5

Hydrocracking of Isooctane

	Rate of isooctane conversion Specific: 10^{-7} mol/g · s Intrinsic: 10^{-3} molec/atom met · s	
Catalyst	Specific rate	Intrinsic rate
RuKY	10	3
RuHY	45	13.7
RuKHYd	114	63.3
RuHYd	132	70.0
RuS_2	0	0

Note. 573 K, $P_{tot} = 0.1$ MPa, $P_{H_2S} = 2.5$ kPa, $P_{isooctane} = 2.3$ kPa.

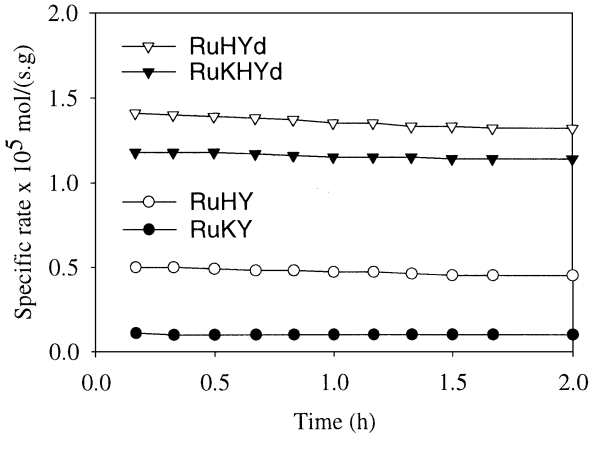

FIG. 9. Isooctane conversion rates for mixtures of various RuY catalysts and RuS_2; weight ratio, RuS_2/RuY = 20.

in the zeolites would probably permit a good balance with the acid properties to be achieved.

As can be seen from Table 5, the rate of isooctane conversion, which is directly related to the catalyst acidity, decreases in the order

$$\text{RuHYd} > \text{RuKHYd} > \text{RuHY} \gg \text{RuKY}.$$

This order of acidity is in agreement with the results deduced from IR spectroscopy.

Hydrogenation of Tetralin

For tetralin hydrogenation, the experimental conditions were chosen in order to avoid thermodynamic equilibrium, which would favor the dehydrogenation of tetralin to form naphthalene, and to obtain a relatively low conversion (less than 15%) of tetralin to hydrogenated products. At these low conversions, high selectivities (≈90%) toward the hydrogenation products *cis*- and *trans*-decalin are observed. Small quantities of isomerization products are also detected which could probably be methylindans from the isomerization of tetralin and isomerization of one or two of the rings of decalin into methylcyclopentanes. After a first period of deactivation, all the catalysts deactivate very slowly and approximately at the same rate. Consequently, the specific rates were measured after 18 h on stream.

The activities per gram of catalyst (specific activities) and per metal atom (intrinsic activities) are reported in Table 6. The hydrogenation activities of RuY-zeolite catalysts were found to be much higher than that of the conventional $NiMo/Al_2O_3$ catalyst with the exception of RuKY catalyst which exhibited a very low activity. The specific activities were found to decrease in the order

$$\text{RuHYd} > \text{RuHY} > \text{RuKHYd} \gg \text{NiMo/Al}_2\text{O}_3 > \text{RuKY},$$

whereas the intrinsic activities decrease in a slightly modified ranking:

$$\text{RuHYd} > \text{RuKHYd} > \text{RuHY} \gg \text{RuKY} \sim \text{NiMo/Al}_2\text{O}_3.$$

TABLE 6

Catalytic Properties in Tetralin Hydrogenation of the RuY Catalysts, Ruthenium Sulfide Supported on Alumina, and a Conventional NiMo Industrial Catalyst

	Rate of tetralin hydrogenation Specific: 10^{-7} mol/g · s Intrinsic: 10^{-3} molec/atom met · s	
Catalyst	Specific rate	Intrinsic rate
$NiMo/Al_2O_3$	1.05	0.11
RuKY	0.39	0.12
RuHY	78.7	24.1
RuKHYd	55.9	31.4
RuHYd	98	52.1
Ru/Al_2O_3	0.6	0.09

Note. Test: $T = 573$ K, $P_{tot} = 4.5$ MPa, $P_{H_2S} = 84.4$ kPa, $P_{tet} = 2.7$ kPa.

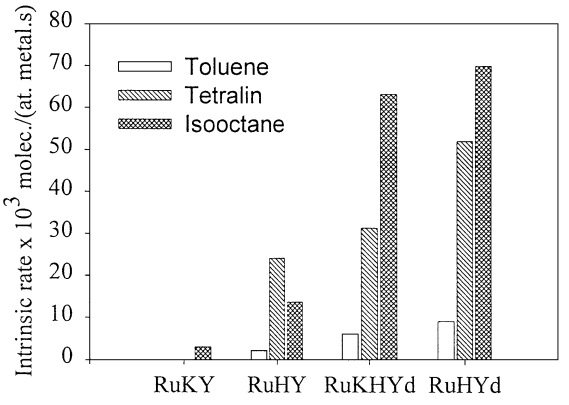

FIG. 10. Correlation of the isooctane conversion rates with the tetralin and toluene hydrogenation rates on the various RuY catalysts.

The classification of the intrinsic activities obtained for the hydrogenation of tetralin and that obtained for the hydrocracking of isooctane correlate well (Fig. 10).

Hydrogenation of Toluene

The hydrogenation of toluene, which is a smaller molecule than tetralin, was investigated in order to determine whether or not the acidity is the main factor modifying the hydrogenating properties of RuY zeolites. The catalyts of the present study presenting various textural properties, some diffusion problems inside the channels of the nondealuminated supports might modify the ranking of activity.

The experimental conditions were chosen to be away from the thermodynamic equilibrium and to obtain a low conversion (less than 15%). The major product was methylcyclohexane with a 50% selectivity. The others were isomerization products such as ethylcyclopentane, methylcyclopentane, and dimethylcyclopentanes. The specific and intrinsic activities are reported in Table 7. The specific activities found in toluene hydrogenation are about 10 times lower than those found in tetralin hydrogenation because of the higher aromaticity and therefore higher stability of toluene compared to tetralin.

They both decrease in the order

$$\text{RuHYd} > \text{RuKHYd} > \text{RuHY} \gg \text{RuKY} \sim \text{NiMo/Al}_2\text{O}_3.$$

The ranking of the intrinsic rates in toluene hydrogenation is identical to that found in the hydrogenation of tetralin and correlates well with the results obtained in the conversion of isooctane (Fig. 10).

TABLE 7

Hydrogenation of Toluene

Catalyst	Rate of toluene hydrogenation Specific: 10^{-7} mol/g · s Intrinsic: 10^{-3} molec/atom met · s	
	Specific rate	Intrinsic rate
$NiMo/Al_2O_3$	0.47	0.049
RuKY	0.11	0.035
RuHY	7.0	2.14
RuKYd	10.9	6.12
RuHYd	17.2	9.15

Note. Test: 573 K, $P_{tot} = 4.5$ MPa, $P_{H_2S} = 84.4$ kPa, $P_{toluene} = 4.8$ kPa.

DISCUSSION

The variation of the properties of metal particles dispersed in zeolites for hydrogenation reactions was studied by many authors. Figueras *et al.* (30) found that the activities of PdY zeolites for benzene hydrogenation were enhanced when Brønsted sites or multivalent cations were present. Thus the turnover frequencies in PdHY, PdLaY, and PdCeY zeolites are 2.5 times larger than in PdNaY and 4 times larger than in Pd/Al_2O_3 or Pd/SiO_2 catalysts. It was proposed that palladium in interaction with electron-acceptor sites is electron deficient and tends to behave like rhodium which is more active than palladium for this particular reaction.

Naccache *et al.* (31) found that the rate of cyclopropane hydrogenation at 295 K was 100 times faster on PtNaY zeolite than on Pt/Al_2O_3 or Pt/SiO_2 catalysts. An additional threefold rate increase was observed for PtCeY while Brønsted sites and particle size did not change. According to these authors, the enhanced rates on zeolites would be better explained by the effect of the zeolite electrostatic field destabilizing the strained cyclopropane ring and thus increasing its reactivity than in terms of the electron deficiency of the metal.

De Mallmann and Barthomeuf studied the hydrogenation of benzene on a series of Pt-faujasites covering a whole range of acidic to basic zeolites (3). The turnover frequency decreased by a factor of 2 from PtHY to PtNaY whereas the ν(CO) wavenumber shifted from 2063 to 2049 cm^{-1}. An increase of the Al content and the exchange of protons by Cs^+ led to a very large decrease of the activity (from 109 for PtHY to ~3 for PtCsX). This order followed that of the decreasing cation acidity and of the simultaneous increasing framework oxygen basicity.

On the other hand, the properties of Ru zeolite catalysts for CO hydrogenation were studied by Oukaci *et al.* (32). For the series of RuY catalysts prepared from NH_4Y, LiY, NaY, RbY, and CsY zeolites, the nature of the group IA cations was found to have little effect on the chemisorptive properties, the activity and chain growth probability in CO hydrogenation on Ru metal.

Three main characteristics of the sulfide clusters dispersed in the zeolite are important for the following discussion: (i) their size is small and they are located inside the zeolite, (ii) they are constituted of a RuS_{2-x}-like phase with tiny domains of ruthenium metal, and (iii) within the sensitivity of the various techniques used, they appear identical whatever the nature of the zeolite supports.

In the present study, the variation of catalytic properties is much higher than in all the above examples; a multiplying factor of about 200 is observed between the less active RuKY and the most active RuHYd zeolite. Since the dispersion of the active phase and its nature are similar for all the supports studied, this modification could be ascribed either to the modification of the electronic properties of the ruthenium active phase, as evidenced by infrared spectroscopy, or to the direct action of the electrostatic field inside the zeolite on the reacting molecule. Both effects may intervene simultaneously.

In favor of the first hypothesis, the following arguments could be proposed: (i) The ν(CO) wavenumber (Table 4) varies between 2056 cm^{-1} for RuKY and 2071 cm^{-1} for RuHY, RuHYd, and RuKYd. The activities for tetralin and toluene hydrogenation follow the same trend, a large difference being observed between RuKY and the other catalysts and a much smaller one within the series of the most active (a factor of 2 or 3 in activity was evidenced between RuHYd and RuHY). (ii) It should be noticed that the activity for tetralin hydrogenation of the ruthenium sulfide supported on the alumina sample is very close to the activity of the RuKY sample as well as the ν(CO) wavenumber (2056 cm^{-1} for RuKY and 2052 cm^{-1} for Ru/Al_2O_3).

This interpretation is also in agreement with the study of Geneste and co-workers (33). Based on a systematic study of the hydrogenation reactions of aromatic compounds and hydrogenolysis of S, N-, and O containing model compounds on molybdenum and tungsten sulfide catalysts, these authors suggested that hydrogenation and hydrogenolysis reactions proceed via different adsorption modes: hydrogenation through horizontal π adsorption and hydrogenolysis through vertical adsorption by the heteroatom. These authors also proposed a dual-site mechanism involving Mo or W at different oxidation levels, the higher oxidation state for the hydrogenation site and the lower one for hydrogenolysis. Following these hypotheses, the electron-deficient character of the ruthenium sulfide cluster when situated in the zeolite acid environment would favor the aromatic adsorption and consequently the hydrogenation would be enhanced.

Nevertheless, it should be mentioned that although the electronic properties of the Ru particles do not change within the series of the three most active catalysts, the

catalytic properties in toluene hydrogenation and tetralin hydrogenation vary by a factor of 2 to 3 according to the molecule to be converted. These variations follow the order of acidity determined by the isooctane conversion and by the $\Delta\nu(OH)$ perturbation. One can also speculate on the amplitude of the overall observed effect which is much larger than for all the other examples quoted above. The adsorption of the aromatic molecules on the acidic sites would increase locally the concentration of reactants around the active phase and therefore increase the rate of the hydrogenation reaction. As shown by electron microscopy the ruthenium sulfide particles are well embedded in the zeolite lattice and in close vicinity to the acidic sites formed either during the sulfidation-reduction step of the ruthenium-exchanged zeolite or present on the support itself. Thus, at that time, it may be concluded that both modifications of the electronic properties of the ruthenium phase and concentration effect may play a role in the enhancement of the hydrogenation properties.

CONCLUSION

The results presented in this paper provide evidence that the nature of the zeolite used to disperse ruthenium sulfide clusters has a marked influence on their catalytic and electronic properties. This effect may be compared to the already observed influence of the zeolite environment on transition metal particles. The ruthenium sulfide catalysts prepared in acidic zeolite present outstanding catalytic properties for the hydrogenation of aromatics in the presence of a high concentration of H_2S (~2%) in the reactant mixture. This represents a much higher concentration of sulfur compounds than the thiotolerant metal catalysts, proposed by the catalysts manufacturers for the hydrogenation of gas oil cuts, can support to keep a reasonable activity.

ACKNOWLEDGMENTS

This work was carried out within the framework of the programme Hydrogenation of Aromatics supported by ELF, IFP, TOTAL, and CNRS-ECOTECH. We thank the European Community for a Human Capital and Mobility Program Fellowship granted to V.K. We are indebted to our colleagues of the Zeolite groups at IRC and Laboratoire de Réactivité de Surface for many fruitful discussions.

REFERENCES

1. Sachtler, W. H. H., and Zhang, Z., *Adv. Catal.* **39**, 129 (1993).
2. Gallezot, P., *Catal. Rev.-Sci. Eng.* **20**, 121 (1979).
3. de Mallmann, A., and Barthomeuf, D., *J. Chim. Phys.* **87**, 535 (1990).
4. Barthomeuf, D., *Catal. Rev.-Sci. Eng.*, in press (1996).
5. Dalla Betta, R. A., and Boudart, M., *in* "Proceedings, Int. Congr. Catal., Miami" (J. H. Hightower, Ed.), p. 1329, 1973.
6. Tri, T. M., Candy, J. P., Gallezot, P., Massardier, J., Primet, M., Védrine, J. C., and Imelik, B., *J. Catal.* **79**, 396 (1983).
7. Leglise, J., Janin, A., Lavalley, J. C., and Cornet, D., *J. Catal.* **114**, 388 (1988).
8. Leglise, J., Manoli, J. M., Potvin, C., Djega-Mariadassou, G., and Cornet, D., *J. Catal.* **152**, 275 (1995).
9. Welters, W. J. J., Vorbeck, G., Zandbergen, H. W., de Haan, J. W., de Beer, V. H. J., and van Santen, R. A., *J. Catal.* **150**, 155 (1994).
10. Cid, R., Villasenor, J., Orellana, F., Fierro, J. L. G., and Lopez Agudo, A., *Appl. Catal.* **18**, 357 (1985).
11. Harvey, T. G., and Matheson, T. W., *J. Catal.* **101**, 253 (1986).
12. Zotin, J. L., Cattenot, M., Portefaix, J. L., and Breysse., M., *Bull. Soc. Chim. Belg.* **104**, 213 (1995).
13. Moraweck, B., Bergeret, G., Cattenot, M., Kougionas, V., Geantet, C., Portefaix, J. L., Zotin, J. L., and Breysse, M., *J. Catal.* **165**, 45 (1997).
14. Welters, W. J. J., Koranyi, T. I., de Beer, V. J. H., and van Santen, R. A., *in* "New Frontiers in Catalysis" (L. Guczi, F. Solymosi, and P. Tétényi, Eds.), Vol. C, p. 1931. Akademiai Kiado, Budapest, 1993.
15. Welters, W. J. J., Ph.D. thesis. Eindhoven University of Technology, 1994.
16. Kougionas, V., Cattenot, M., Zotin, J. L., Portefaix, J. L., and Breysse, M., *Appl. Catal. A: General* **124**, 153 (1995).
17. Stanislaus, A., and Cooper, B. H., *Catal. Rev.-Sci. Eng.* **36**, 75 (1994).
18. Cooper, B. J., and Donnis, B. B. L., *Appl. Catal. A: General* **137**, 203 (1996).
19. Bourdillon, G., Gueguen, C., and Guisnet, M., *Appl. Catal.* **61**, 123 (1990).
20. De Los Reyes, J.A., Göbölös, S., Vrinat, M., and Breysse, M., *Catal. Lett.* **5**, 587 (1990).
21. Lacroix, M., Boutarfa, N., Guillard, C., Vrinat, M., and Breysse, M., *J. Catal.* **120**, 473 (1989).
22. Maache, M., Ph.D. thesis. Caen, France, 1993.
23. Gruver, V., and Fripiat, J., *J. Phys. Chem.* **98**, 8549 (1994).
24. Hadjiivanov, K., Lavalley, J. C., Lamotte, J., Saint Just, J., and Che, M., to be published.
25. Cairon, O., Ph.D. thesis. Caen, France, 1995.
26. Barthomeuf, D., *Mater. Chem. Phys.* **17**, 49 (1987).
27. Makarova, M. A., Garforth, A., Zholobenko, V. L., Dwyer, J., Earl, G. S., and Rawlence, D., *Stud. Surf. Sci. Catal.* **84**, 365 (1994).
28. de Mallmann, A., and Barthomeuf, D., *Stud. Surf. Sci. Catal.* **46**, 429 (1989).
29. De Los Reyes, J. A., Vrinat, M., Breysse, M., Mauge, F., and Lavalley, J. C., *Catal. Lett.* **13**, 213 (1992).
30. Figueras, F., Gomez, R., and Primet, M., *Adv. Chem. Ser.* **121**, 480 (1973).
31. Naccache, C., Kaufherr, N., Dufaux, M., Bandiera, J., and Imelik, B., *in* "Molecular Sieves II" (J. R. Katzer, Ed.), p. 538. Am. Chem. Soc., Washington, DC, 1977.
32. Oukaci, R., Wu, J. C. S., and Goodwin, J. G., Jr., *J. Catal.* **107**, 471 (1987).
33. Moreau, C., and Geneste, P., *in* "Theoretical Aspects of Heterogenous Catalysis" (J. B. Moffat, Ed.), p. 256. Van Nostrand–Reinhold, New York, 1990.